Attention to 3-D Shape, 3-D Motion, and Texture in 3-D Structure from Motion Displays

Hendrik Peuskens[1], Kristl G. Claeys[1,2], James T. Todd[3], J. Farley Norman[4], Paul Van Hecke[5], and Guy A. Orban[1]

Abstract

■ We used fMRI to directly compare the neural substrates of three-dimensional (3-D) shape and motion processing for realistic textured objects rotating in depth. Subjects made judgments about several different attributes of these objects, including 3-D shape, the 3-D motion, and the scale of surface texture. For all of these tasks, we equated visual input, motor output, and task difficulty, and we controlled for differences in spatial attention. Judgments about 3-D shape from motion involve both parietal and occipito-temporal regions. The processing of 3-D shape is associated with the analysis of 3-D motion in parietal regions and the analysis of surface texture in occipito-temporal regions, which is consistent with the different behavioral roles that are typically attributed to the dorsal and ventral processing streams. ■

INTRODUCTION

We live in a three-dimensional (3-D) world; we see and interact with 3-D objects. Because the retinal image is flat, the brain has to recreate the third dimension. Several different aspects of optical structure are known to provide perceptually salient information about an object's 3-D form. One especially powerful source of information is provided by the optical deformations that occur when objects are observed in motion (Todd & Norman, 1991; Ullman, 1979; Wallach & O'Connell, 1953). Recent imaging work in both humans (Kriegeskorte et al., 2003; Paradis et al., 2000; Orban, Sunaert, Todd, Van Hecke, & Marchal, 1999) and monkeys (Sereno, Trinath, Augath, & Logothetis, 2002; Vanduffel et al., 2002) has shown that motion displays evoking the perception of a 3-D object activate a range of cortical areas, including lateral occipital, parietal, and occipito-temporal visual regions. This widespread activation in passive subjects has been considered as evidence that 3-D shape is processed in both the dorsal and ventral streams. It is important to keep in mind, however, that moving displays produce several distinct perceptual attributes. For example, one possible interpretation of the pattern of activation during passive viewing is that the dorsal pathway analyzes the 3-D motion of a moving object, whereas the ventral pathway is primarily involved in the analysis of 3-D shape (Grünewald, Bradley, & Andersen, 2002; Goodale & Milner, 1992; Ungerleider & Mishkin, 1982). Such a division of labor would be in line with the traditional distinction between the attributes that are processed by the ventral and dorsal pathways (Aguirre & D'Esposito, 1997; Haxby et al., 1994; Ungerleider & Mishkin, 1982). Alternatively, 3-D shape might be processed in both the dorsal and ventral stream. In order to investigate these possibilities we have performed an active experiment in which subjects made judgments about several different attributes (Corbetta, Miezin, Dobmeyer, Shulman, & Petersen, 1991) of moving objects, including their 3-D shapes and 3-D motions.

In all conditions, subjects viewed successive animation sequences of randomly shaped textured objects rotating about a vertical axis slanted in depth. In the three main conditions, they made same–different judgments about the 3-D shape, the 3-D axis of rotation, or the spatial scale of the texture (Figure 1). Whereas the 3-D shape and 3-D motion conditions required the processing of the optic flow (Norman, Todd, & Philips, 2001), the texture judgments did not. Two additional control conditions were included using exactly the same displays, in which subjects were required to detect a slight dimming in the luminance of either the central or peripheral regions of the moving objects. These controls were added because a pilot experiment had revealed that judgments of 3-D shape or motion involved the whole object, whereas texture judgments were primarily based on its central part, and it is known that differences in distribution of visuospatial attention can influence retinotopic patterns of activation in visual cortex (Peuskens, Sunaert, Dupont, Van Hecke, & Orban, 2001; Brefczynski & De Yoe, 1999; Tootell et al., 1998). The visual input, the two alternative forced-choice paradigm, and motor response were identical over all five conditions. All that changed was the

[1]K.U.Leuven, Medical School, [2]University of Antwerpen, [3]The Ohio State University, [4]Western Kentucky University, [5]UZ Gasthuisberg

© 2004 Massachusetts Institute of Technology

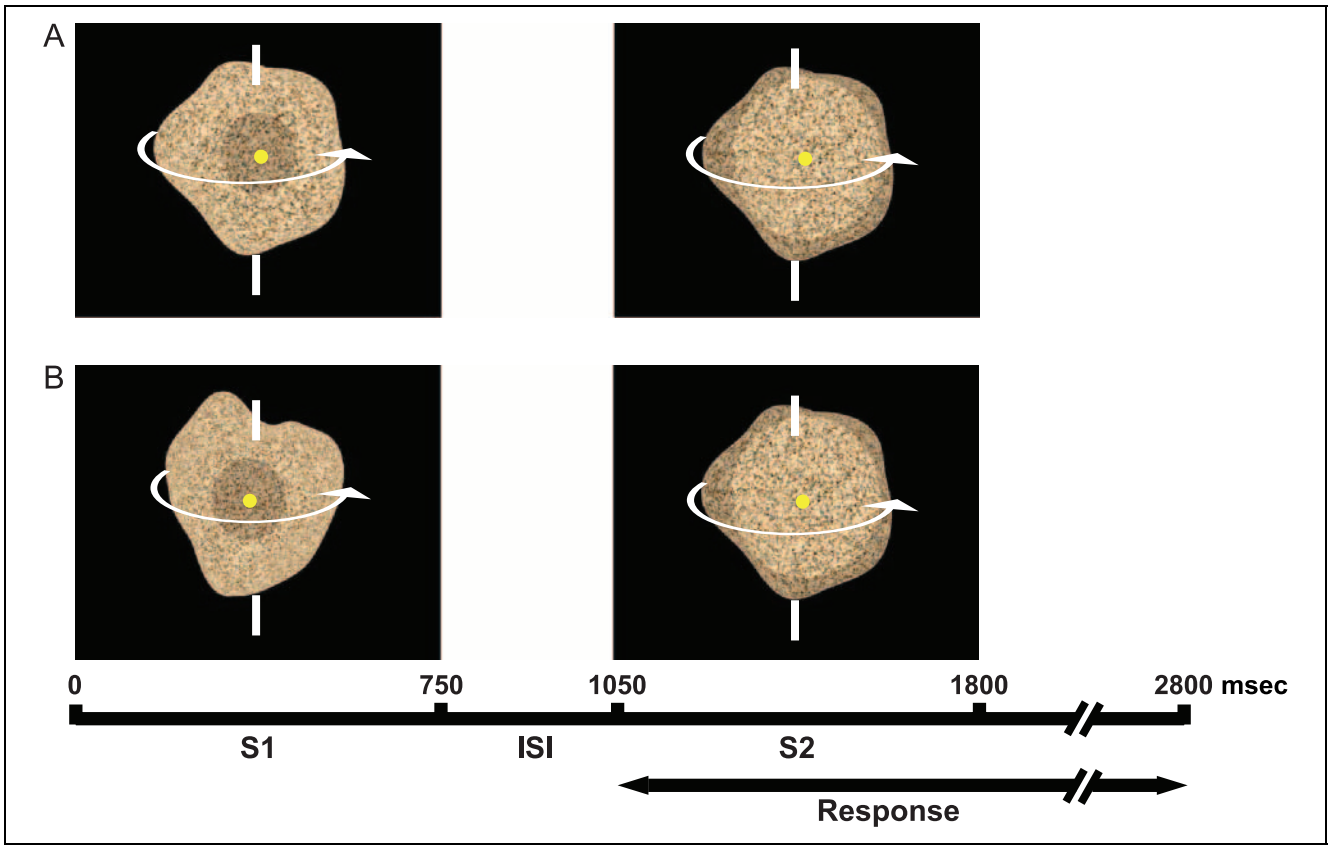

Figure 1. Schematic representation of texture judgment trials: same trial (A) and different trial (B). Stimulus 1 and 2 show the central and peripheral dimming, respectively. The timing of the stimulus presentations and response period is indicated. The vertical line indicates the axis of rotation, which was slanted in the z direction (outside the plane of this figure).

particular stimulus attribute the observers were required to judge**,** which has been shown to enhance the tuning of neurons selective for the attended attribute (Treue & Martinez Trujillo, 1999). Finally, a fixation-only condition was included as a low-level reference condition. To further rule out effects of spatial attention, an additional control experiment was performed in which portions of the depicted objects were masked, thus forcing observers to focus their attention either centrally or peripherally in order to perform the required judgments.

RESULTS

Behavioral Performance

Average performance over the different conditions of the main experiment ranged from 81% to 84% correct, which was not significantly different, $F(4,56) = 0.64$, $p = .63$. In the control experiment average performance was 85% correct for the three peripheral conditions and ranged between 82% and 84% for the central conditions. Subjects maintained fixation well during the active epochs; eye blinks were allowed and occurred typically on trial termination. Eye movements and blinks were counted and compared over the different conditions of the main experiment. No significant difference in eye movement counts was found between the active epochs (Friedman Fr = 7.8114, $p = .098$). During passive fixation epochs, blinks and saccades were more frequent (total average of 15.9/min) as compared to during active epochs (7–9.4/min).

Group Analysis of Main Imaging Experiment: Activation Sites Specific to Discrimination of Different Attributes

In the principal analysis of the main experiment, we compared directly the MR activity averaged over subjects in one discrimination task to that in each of the two others. We use a color code (Figure 2) to visualize the results of the main experiment, with red indicating regions involved in 3-D shape judgments more than in the two other discriminations, yellow for 3-D motion-specific regions, and blue for texture-specific regions. Intermediate selectivity is indicated by intermediate colors; for example, orange indicates voxels where both 3-D shape and 3-D motion judgments differed significantly from texture judgments. This activation pattern indicates that the regions involved with judgments of 3-D shape are located both ventrally and dorsally. The regions involved

with 3-D motion judgments, in contrast, are all located in the lateral occipito-temporal and parietal cortex, whereas regions involved with judgments of texture are all confined to the ventral occipito-temporal cortex.

Within this activation pattern, only 13 regions reached the strict significance criterion (see Methods) and are described further as specific regions (Table 1). Ten of these regions were symmetric in the two hemispheres, while three were lateralized in a single hemisphere. Three bilateral regions, numbered 2–4 in Figure 2, were specific only for 3-D shape: lateral occipital sulcus (3, LOS, Orban et al., 1999), inferior temporal gyrus (2, ITG), and posterior intraparietal sulcus (4, IPS). Two other bilateral regions (labeled 1 and 5 in Figure 2) were involved in both 3-D shape and 3-D motion judgments: hMT/V5+ (Tootell et al., 1995; Dupont, Orban, De Bruyn, Verbruggen, & Mortelmans, 1994; Watson et al., 1993; Zeki et al., 1991) and anterior IPS. Local maxima for hMT/V5+ in the main subtractions (R: 54, −60, 0; L: −45, −72, 3) correspond closely to those from the motion localizer runs (R: 51, −66, 3; L: −54, −72, 3).

No region was found to be specific for just 3-D-motion judgments. On the other hand, several regions were involved in texture judgments. Many of these were located in the posterior occipital cortex, at the level of the early retinotopic regions. Since these regions (indicated by a black dashed curve in Figure 2) were more active in the dimming central condition than the dimming peripheral one, their activation was considered to reflect visuospatial attention differences rather than texture processing as such. This common activation of early visual regions in texture judgments and in central dimming detection agrees with our psychophysical pilot results. The remaining texture-selective regions included the right posterior and middle collateral sulcus (labeled 8 and 6, respectively, in Figure 2) as well as the left middle lingual gyrus (labeled 7 in Figure 2). The texture-selective regions in the right hemisphere were also activated to some degree by judgments of 3-D shape, whereas that in the left hemisphere was additionally engaged by judgments of 3-D motion. Although more voxels in Figure 2 were related to texture judgments (purple voxels), these did not meet the criterion for defining specific regions.

Figures 3 and 4 show the localization of 8 of the 13 activation sites (Figure 3), as well as their activity in the five discrimination and detection tasks (Figure 4). For the bilateral sites (three 3-D shape regions and two 3-D shape/3-D motion regions) only one of the two symmetric sites is illustrated. The fixation condition is

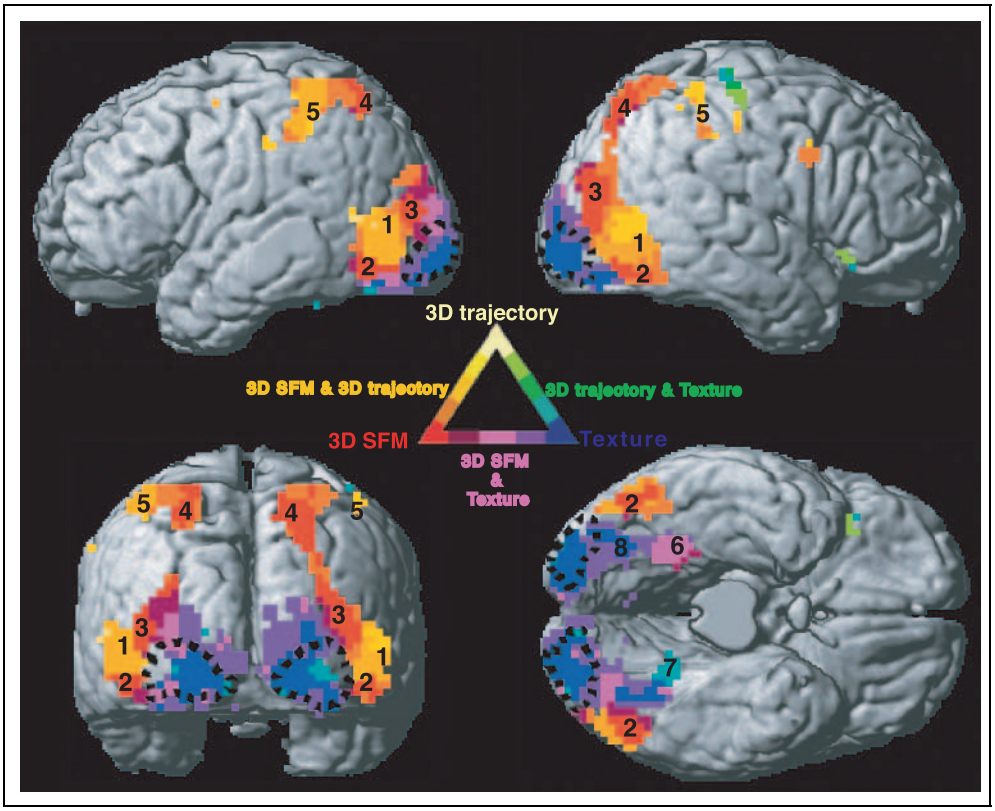

Figure 2. The patterns of activation revealed by a random-effects analysis, thresholded at $p < .001$ uncorrected for multiple comparisons, and rendered on a standard brain template. Numbers denote local maxima in areas significant at $p < .05$ corrected for multiple comparisons. Color scale indicates relative activation in three different conditions: attention to 3-D shape from motion (red), to orientation of rotation axis (3-D motion, pale yellow) or to texture (blue). Dotted outline in the occipital lobe demarcates brain regions for which a significant effect of visuospatial attention was found in the comparison between the detection of central and peripheral dimming. In this area, only texture-specific voxels were found. Numbers indicate specific regions: 1: hMT/V5+, 2: inferior temporal gyrus, 3: lateral occipital sulcus, 4: posterior intraparietal sulcus, 5: anterior intraparietal sulcus, 6: right middle collateral sulcus, 7: left middle lingual gyrus, 8: right posterior collateral sulcus.

Table 1. Localization of the Specific Regions (n = 13) in the Main Experiment with Z Scores (Random Effects) in the Group Analysis and Number of Subjects Showing Significant Activation

A. Shape-Specific Regions

						No. of Subjects[a]		
	x	*y*	*z*	*SM*	*ST*	*SM*	*ST*	Both Tasks
R LOS	42	−78	12	3.37	**4.99**	12/15	12/15	11/15
L LOS	−36	−90	12	**4.45**	3.5	11/15	9/15	9/15
R ITG	51	−69	−12	3.63	**4.64**	11/15	13/15	11/15
L ITG	−48	−66	−12	4.22	**4.45**	12/15	11/15	10/15
R posterior IPS	21	−72	54	3.66	**4.86**	12/15	15/15	12/15
L posterior IPS	−18	−60	63	3.55	**4.35**	12/15	12/15	10/15

B. Shape- and Motion-Selective Regions

						No. of Subjects		
	x	*y*	*z*	*ST*	*MT*	*ST*	*MT*	*Both Tasks*
R hMT/V5+	54	−60	0	3.40	**4.34**	12/15	14/15	12/15
L hMT/V5+	−45	−72	3	3.4	**4.86**	12/15	14/15	12.15
R anterior IPS	36	−33	42	3.26	4.14	12/15	14/15	12/16
L anterior IPS	−42	−42	51	3.12	**4.79**	11/15	13/15	9/15

C. Texture-Specific Regions

						No. of Subjects		
	x	*y*	*z*	*TS*	*TM*	*TS*	*TM*	*Both Tasks*
R middle collateral sulcus	30	−45	−15	−0.1	3.55[b]	8/15	11/15	5/15
L middle lingual gyrus	−18	−51	−18	**4.45**	1.26	12/15	6/15	4/15
R posterior collateral sulcus	36	−81	−15	3.26	**4.86**	9/15	11/15	7/15

[a]Single subjects reaching $p < .001$ uncorrected.

Bold: $Z > 4.31$, $p < .05$ corrected (random effects).

SM = 3-D shape compared to 3-D motion; ST = 3-D shape compared to texture; MT = 3-D motion compared to texture; TS = texture compared to 3-D shape; TM = texture compared to 3-D motion.

[b]SM: $Z = 4.45$.

not indicated in the activity profiles (Figure 4), since the analysis ensured that all regions were more active in the task conditions than during simple fixation. For most shape-selective regions (1–6) the MR signals during shape discrimination also differed significantly from those recorded in the detection conditions, with the exception of posterior IPS. In all regions, including the texture-selective ones, the activity during the two detection tasks was similar, indicating that none of the main effects in these regions can be due to variations in spatial attention (Nobre et al., 1997; Vandenberghe et al., 1996; Corbetta, Miezin, Shulman, & Petersen, 1993; Corbetta et al., 1998).

Group Analysis of Main Imaging Experiment: Activation Sites Common to All Discrimination Tasks

The group analysis of the main experiment has thus far concentrated on regions specifically involved in one or two same–different tasks. Theoretically, a number of cortical regions could also be engaged in all three discrimination tasks. Only four regions (Figure 5) were significantly ($p < .05$ corrected) engaged by all three tasks: Two local maxima were located in the right ITG, the two other in the right middle fusiform gyrus and right inferior parietal lobule. The two right ITG sites

were proportionally more engaged by the 3-D shape judgments than the two other judgments, in keeping with their proximity to the ITG site specific for 3-D shape judgments. This involvement of right ITG in temporal same–different tasks is in agreement with a string of articles from this laboratory indicating the

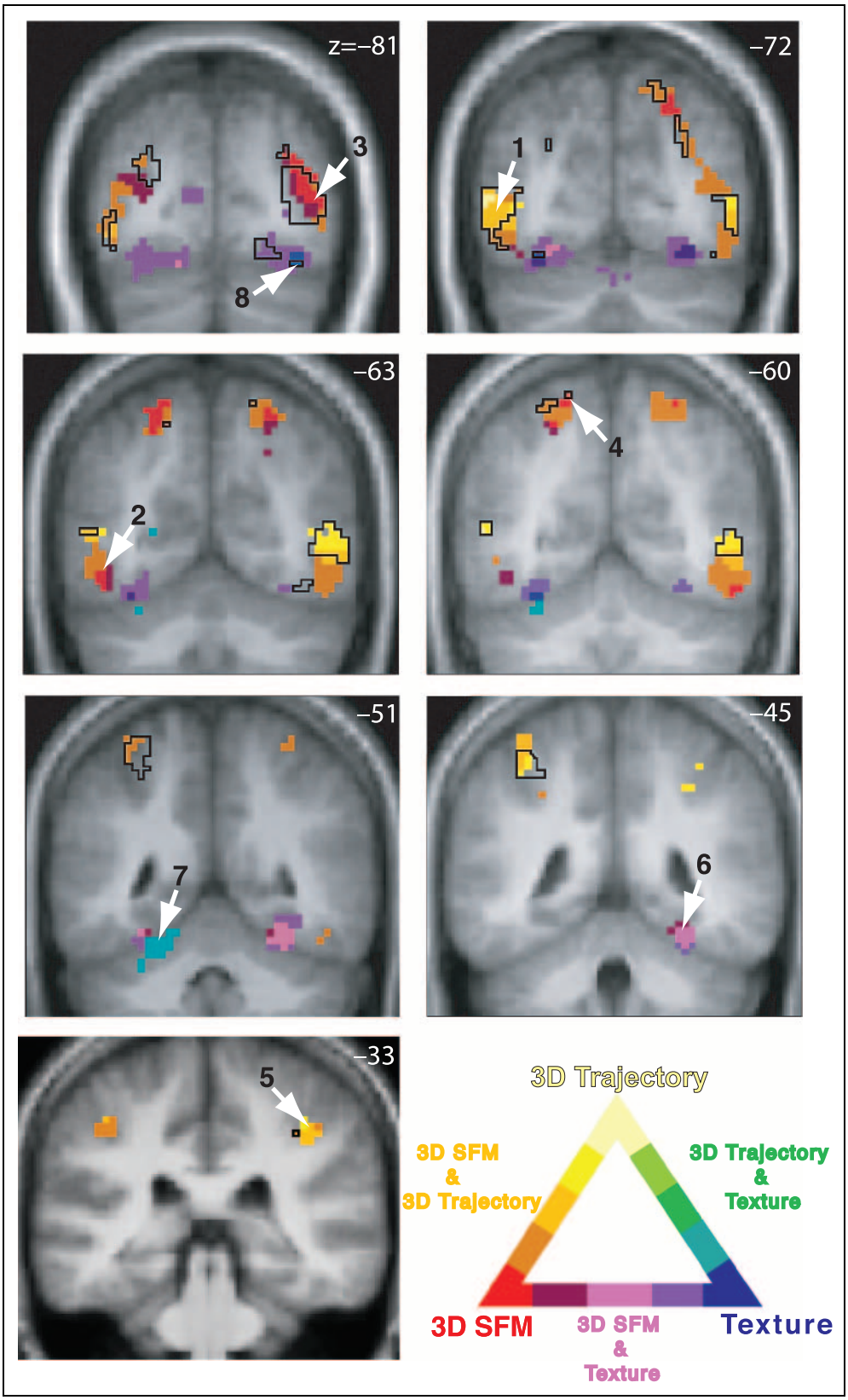

Figure 3. Coronal sections of the average brain of 15 subjects with activation patterns rendered using the same color scale as Figure 2. The black outline demarcates activation obtained in the motion localizer scans ($p < .0001$ uncorrected for multiple comparisons). The y coordinate of sections is indicated in the top right corner of each panel. Numbering as in Figure 2.

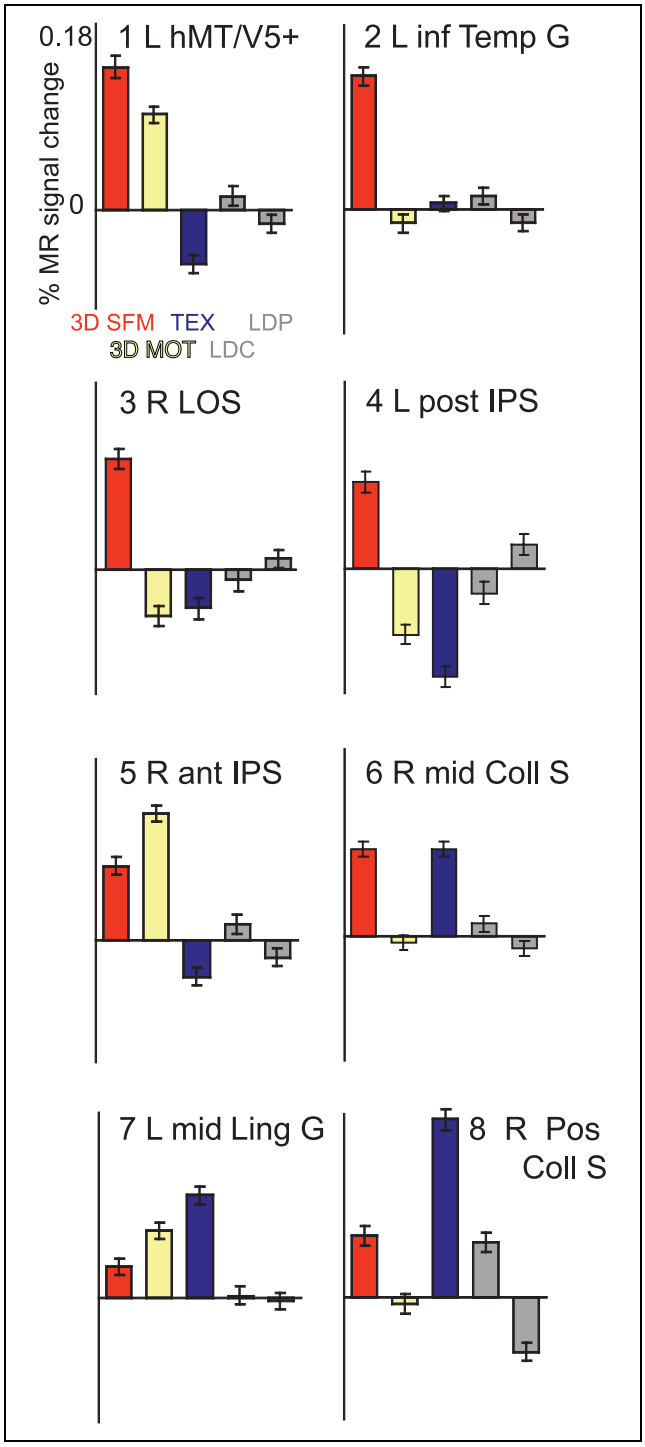

Figure 4. Activity profiles (group analysis) show percent MR signal change compared to the average of the dimming control tasks. Error bars: *SEM* from fixed effect group analysis; numbering as in Figures 2 and 3; 1: hMT/V5 (−45, −72, 3); 2: inferior temporal gyrus (−48, −63, −12); 3: lateral occipital sulcus (42, −81, 9); 4: posterior intraparietal sulcus (−18, −60, 66); 5: anterior intraparietal sulcus (36, −33, 42); 6: right middle collateral sulcus (30, −45, −15); 7: left middle lingual gyrus (−18, −51, −18); 8: right posterior collateral sulcus (36, −81, −15). 3-D SFM = 3-D shape from motion task; 3-D MOT = orientation of rotation axis task; TEX = texture task; LDC = luminance dimming detection in center; LDP = luminance dimming detection in periphery.

involvement of this region in successive discrimination of orientation (Fias, Dupont, Reynvoet, & Orban, 2002; Cornette, Dupont, Bormans, Mortelmans, & Orban, 2001; Faillenot, Sunaert, Van Hecke, & Orban, 2001; Orban, Dupont, Vogels, Bormans, & Mortelmans, 1997), of direction (Cornette et al., 1998), and of speed (Orban et al., 1998).

Single-Subject Analysis: Individual Activation Patterns

In addition to the group analysis, we performed single-subject analyses of the main experiment. While the random effect analysis ensures that the results described so far can be generalized to all young and healthy humans, it provides no information about variability across subjects. Single-subject analyses also make it possible to compute the activity profile of cortical regions defined by the motion localizer or shape localizer. Figure 6 shows the activation pattern using the color code of Figure 2 on the rendered brains of five individual subjects. Two subjects were chosen for the strength of their activation pattern, the three others because the LO localizer was tested in these subjects. Motion localizer tests were available for all subjects, but rather than indicating all motion-sensitive regions, only two of them, hMT/V5+ and dorsal intraparietal sulcus anterior (DIPSA) (Sunaert, Van Hecke, Marchal, & Orban, 1999), are indicated in Figure 6. In general, the activation pattern in the single subjects agrees with the group pattern (Figure 2), but it is of course much noisier. Given the random effects option pursued in this study, the number of functional volumes sampled in each subject is relatively small according to our own standards (Vanduffel et al., 2002). Despite this variability, 3-D shape-specific and 3-D shape- and 3-D motion-specific regions were observed (at $p < .001$ uncorrected) in more than half the subjects (Table 1). The texture-specific regions are generally defined by a single contrast and, in this case, more than half the subjects showed a significant activation (Table 1). We tested statistically whether subjects for whom a given region was significant for a given subtraction performed better than those for whom this subtraction did not reach significance. After correction for multiple comparison ($n = 14$) none of the region/subtraction combinations were associated with a significant difference in performance. All subjects were naïve to the tasks before being enrolled in the experiment. Hence, the relatively small number of functional volumes sampled per subject is likely to be the primary source of variability among subjects.

Figure 6 also indicates that the pITG region (2) is located below hMT/V5+, while the motion-sensitive region DIPSA is located in between the posterior and anterior IPS regions (4 and 5). The LOS region (3) is

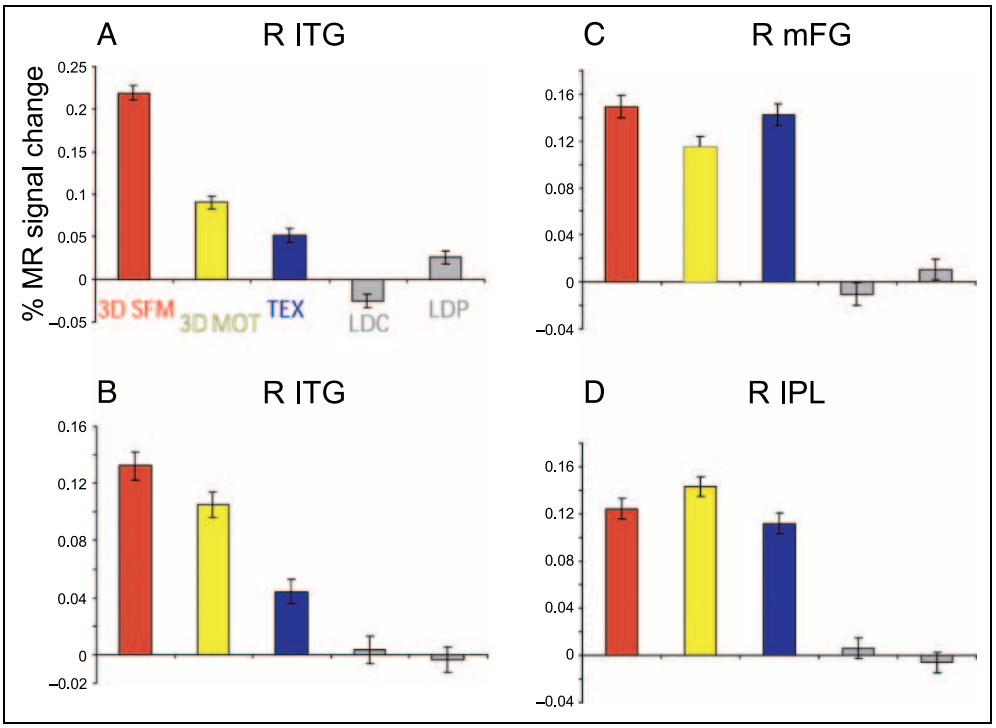

Figure 5. Activity profiles (group analysis) plotting percent MR signal change compared to the average of the dimming control tasks for regions common to the three same–different judgments. Error bars: *SEM* from fixed-effect group analysis. (A) right ITG (54, −57, −12); (B) right ITG (42, −75, −3); (C) right middle fusiform gyrus (39, −39, −24); (D) right inferior parietal lobule (51, −30, 54). Same conventions as Figure 4.

located behind hMT/V5+, but also more dorsal compared to hMT/V5+ and even to the 2-D shape-sensitive LOS region.

Single-Subject Analysis: Involvement of Motion-Sensitive Regions

To investigate the relationship between the regions active in the behavioral tasks and the 2-D motion-sensitive regions, we tested the most significant voxel of motion-sensitive regions, obtained in the motion localizer for its activity in the different behavioral tasks of the main experiment. We concentrated (Figure 7) on four motion-sensitive regions (Sunaert et al., 1999): hMT/V5+, LOS, dorsal intraparietal sulcus medial (DIPSM), and DIPSA. The functional profile of motion-sensitive LOS (Figure 7A) is very similar to that of the LOS region in the group analysis (Figure 4), suggesting that this might be the same region. Human MT/V5+ (Figure 7C) is indeed involved in judgments of both 3-D shape and orientation of the rotation axis, again in agreement with the group result. Additional probing 9 mm above and below the local motion localizer maximum indicated that the dorsal part of the MT/V5 complex is relatively more involved in 3-D motion judgments and the ventral part more in 3-D shape judgments (Figure 7B and D). This ventral part is contiguous to the 3-D shape-specific pITG region. Thus, the dorsoventral gradient across hMT/V5+ from 3-D motion specific dorsally to 3-D shape specific ventrally, is not an effect of smoothing in the group analysis. This transition has also been documented by Kourtzi, Bulthoff, Erb, and Grodd (2002). The motion-sensitive region DIPSM shows a profile similar to that of the posterior IPS region in the group analysis (4). On the other hand, DIPSA has a profile intermediate between that of posterior and of anterior IPS of the group analysis (4 and 5), in agreement with its anatomical position. With respect to the LO complex (Malach et al., 1995, Kourtzi & Kanwisher, 2000), the three 2-D shape-sensitive regions, LOS, pITG, or mFG were, to various degrees, involved in all three discriminations (Figure 8). In fact, these activity profiles are similar to those of the regions involved in all discriminations according to the group analysis (Figure 6).

Control Imaging Experiment: Spatial Attention versus Featural Attention

In all 13 regions specifically engaged by one or two of the same–different judgments, the difference in activity between central and peripheral dimming detection was extremely small, indicating that these regions were not engaged in overt control of spatial attention. This does not exclude the possibility that spatial attention and featural attention interact. For example, the subjects might have attended more to the peripheral parts of the objects in the 3-D motion and 3-D shape judgments than in the texture judgments. To control for different spatial attention demands across the three judgments, we tested all three judgments both with peripheral and central attention focus in the control experiment. To analyze the results of this experiment we made exactly the same contrasts as in Figure 2, but averaged them

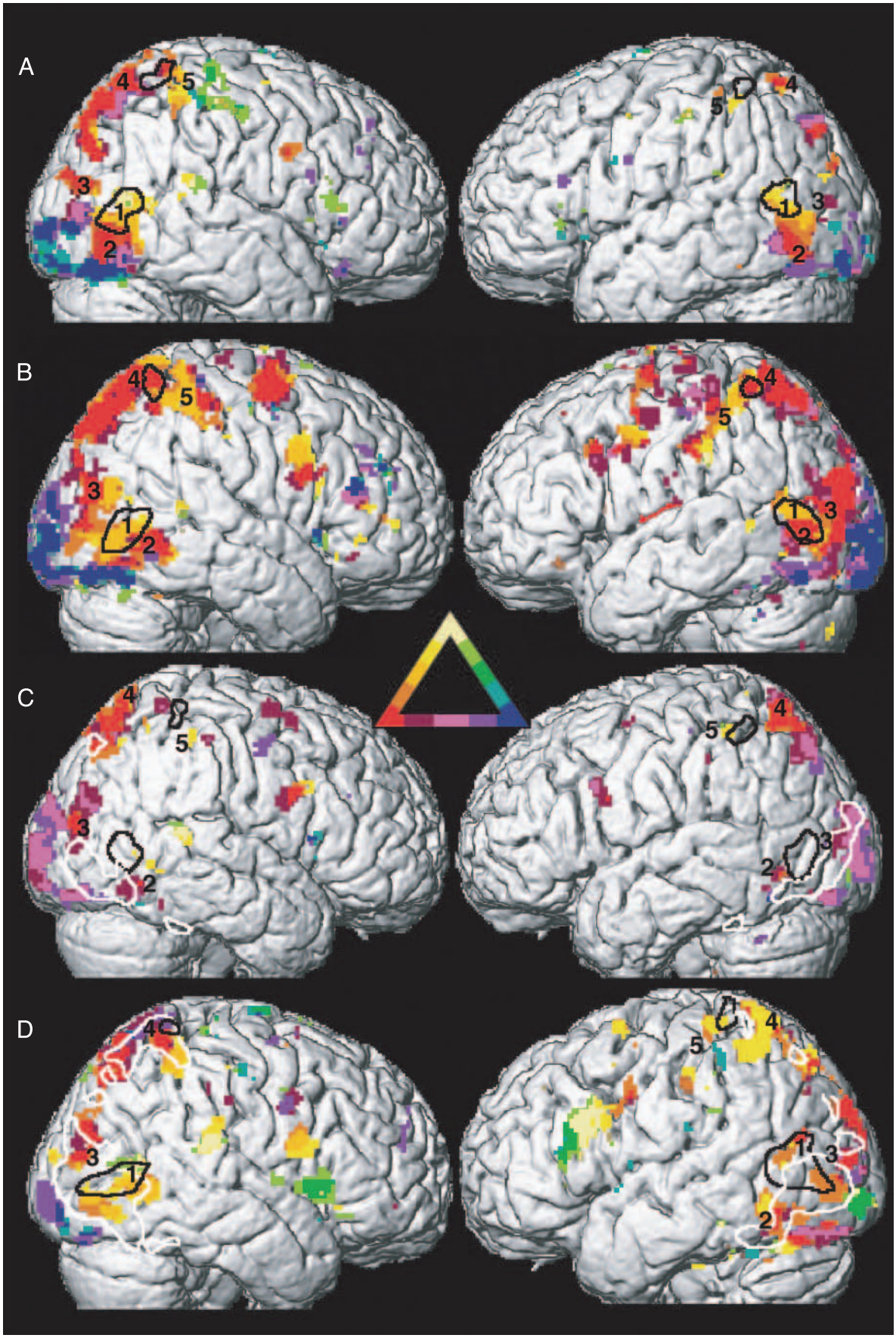
A
B
C
D

over central and peripheral conditions. This yielded the same regions as in the main experiment, with the exception that the middle collateral sulcus region, specific for texture and shape, was now observed bilaterally, increasing the number of specific regions to 14 (Table 2). For each of the 14 regions we tested the interaction between spatial attention and featural attention and it only reached significance ($p < .001$ uncorrected) in hMT/V5+, in which the central judgments evoked more MR activity than the peripheral judgments. Yet, the main effects of featural attention were extremely significant (Table 2). The activity profiles (Figure 9) confirm that the specific engagement of all regions by one or two discrimination tasks is not dependent on the focus of spatial attention. For comparison a region (posterior fusiform gyrus) in which both the spatial attention effects and the difference between texture judgements and 3-D shape or 3-D motion judgements were significant is also shown. This region was located within the black dashed curve at the back of the brain in Figure 2. Finally, the posterior lingual region illustrates a region in which spatial attention had a significant effect in all three tasks. In this region, the activity modulation is complete, indicating that the spatial attention manipulation was very effective.

DISCUSSION

In order to study the effect of attention to different attributes of dynamic 3-D displays, we equated not only visual input, motor response, and performance level, but also, indirectly, the region of space attended. The latter was directly controlled in a separate experiment. Because behavioral purpose (Goodale & Milner, 1992) and cognitive operations (Fias et al., 2002) have been shown to differ between dorsal and ventral pathways, those were kept constant across the discriminations tasks in order to isolate the effect of stimulus attribute on the dorsal/ventral pathway distinction. The results revealed that 3-D shape is processed in both dorsal and ventral pathways, but that 3-D motion is processed predominantly in the dorsal pathway and texture (as quality of an object) is processed exclusively in the ventral pathway. These findings indicate that the two pathways are not completely segregated with respect to the stimulus attributes they process. 3-D shapes are apparently of sufficient biological importance to be processed in both dorsal and ventral streams.

The human MT/V5 complex was engaged by both 3-D shape and 3-D motion judgments but not texture judgments. There is growing evidence from imaging studies that this motion-sensitive complex (Tolias, Smirnakis, Augath, Trinath, & Logothetis, 2001; Vanduffel et al., 2001; Tootell et al., 1995; Dupont et al., 1994; Watson et al., 1993; Zeki et al., 1991) is involved in extracting 3-D structure from motion in humans (Vanduffel et al., 2002; Orban et al., 1999) and also in monkeys (Sereno et al., 2002; Vanduffel et al., 2002). The monkey imaging experiments in which exactly the same stimuli were used in awake monkeys as well as in humans (Vanduffel et al., 2002) indicate that in addition to MT/V5 itself, FST extracts 3-D structure from motion, in agreement with Sereno et al. (2002). Thus, it is likely that in the human complex the homologues of MT/V5 and of FST also contribute heavily to its activation by 3-D structure from motion stimuli. The MR activation of MT/V5 by 3-D structure from motion stimuli establishes a direct link between the activation of hMT/V5+ by 3-D structure from motion and the properties of MT/V5 neurons in monkeys. These neurons have been shown to be selective for the direction of speed gradients, which corresponds to the tilt of a 3-D surface (Xiao, Marcar, Raiguel, & Orban, 1997; see also Bradley, Chang & Andersen, 1998). The present results extend these observations and, for the first time, indicate that this motion information about 3-D structure is actively used when subjects make judgments about 3-D shape. The fact that hMT/V5+ was also engaged by 3-D motion judgments is consistent with the view that hMT/V5+ represents a relative early stage in the processing of dynamic 3-D stimuli, in which the different functional consequences of optic flow are not yet separated. It could be argued that this common engagement of hMT/V5+ by 3-D shape and 3-D motion judgements is due to selection of the whole object (O'Craven, Downing, & Kanwisher, 1999), so that regions processing all of its attributes are activated, even if only a single attribute is attended. This is unlikely since several other regions, including other motion-sensitive regions, are engaged in judgements of 3-D shape, but show no activation for judgements of 3-D motion. Furthermore, the gradient of specificity observed across the hMT/V5+ complex would be difficult to reconcile with the whole object-selection hypothesis.

Judgments of 3-D shape involved both dorsal and ventral regions, contrary to predictions based on the initial distinction between these pathways (Haxby et al., 1994; Ungerleider & Mishkin, 1982). This finding for

Figure 6. The patterns of activation revealed by single-subject analysis, thresholded at $p < .001$ uncorrected for multiple comparisons, and rendered on the subjects' brain (lateral view). (A–C) Right and left hemisphere of Subject 6 (A), Subject 1 (B), and Subject 13 (C). (D) Right hemisphere of Subject 14 and left hemisphere of Subject 15. Color scale (see Figures 2 and 3) indicates relative activation in three different conditions: attention to 3-D shape from motion (red), to orientation of rotation axis (3-D motion, pale yellow), or to texture (blue). Numbers as in Figures 2 and 3. Black outlines: hMT/V5+ and DIPSA ($p < .05$ corrected contour). White outlines: LO complex localizer ($p < .05$ corrected contour).

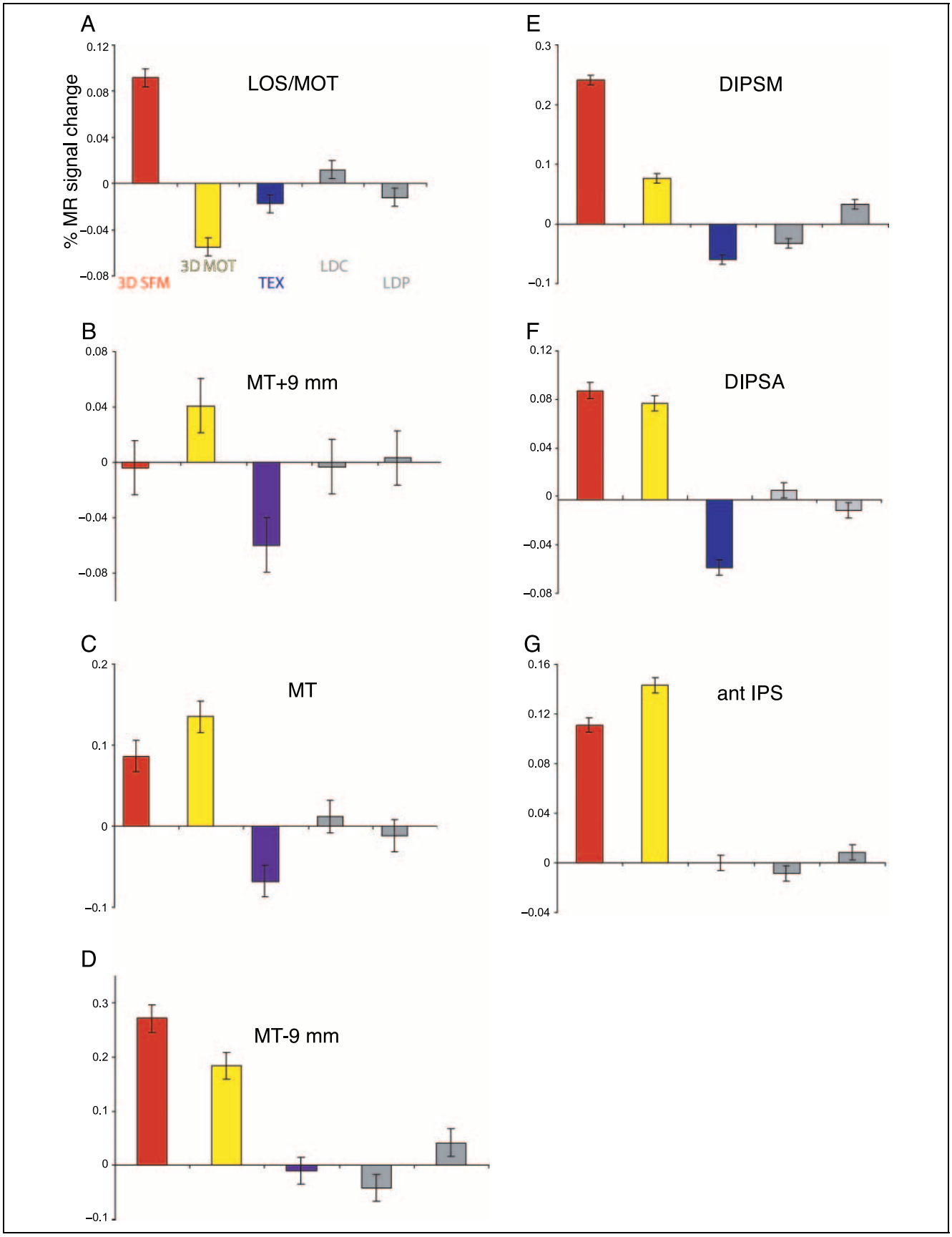
A
LOS/MOT
% MR signal change
0.12
0.08
0.04
0
−0.04
−0.08
3D SFM
3D MOT
TEX
LDC
LDP
B
MT+9 mm
0.08
0.04
0
−0.04
−0.08
C
MT
0.2
0.1
0
−0.1
D
MT-9 mm
0.3
0.2
0.1
0
−0.1
E
DIPSM
0.3
0.2
0.1
0
−0.1
F
DIPSA
0.12
0.08
0.04
0
−0.04
−0.08
G
ant IPS
0.16
0.12
0.08
0.04
0
−0.04

motion-defined shapes is in agreement with an earlier PET study of Faillenot, Toni, Decety, Gregoire, and Jeannerod (1997) using real 3-D objects. It adds to the growing list of imaging studies indicating that 2-D and 3-D shape are processed in both streams (Kriegeskorte et al., 2003; James, Humphrey, Gati, Menon, & Goodale, 2002; Sereno et al., 2002; Vanduffel et al., 2002; Paradis et al., 2000; Orban et al., 1999; Grill-Spector et al., 1998; Van Oostende, Sunaert, Van Hecke, Marchal, & Orban, 1997). All previous experiments involving 3-D shape were performed in passive subjects, however, so it is difficult to determine the precise aspects of the stimulus displays that may have been responsible for the cerebral activation pattern. The present study using active judgments provides conclusive evidence that both dorsal and ventral streams are actively involved in the perception of 3-D shape. While the role of inferotemporal cortex in processing visual shape information has long been established (Kovács, Vogels, & Orban, 1995; Logothetis & Pauls, 1995; Tanaka, Saito, Fukada, Moriya, 1991; Gross, Rocha-Miranda, & Bender, 1972), single-cell studies have also indicated that parietal neurons can actively process shape information (Sereno & Maunsell, 1998).

The regional distribution of neural activation for 3-D shape from motion judgments is relatively similar to the pattern of activation in passive experiments (Vanduffel et al., 2002; Orban et al., 1999), although the ventral involvement is clearer in 3-D shape discrimination than in the passive case. The ventral region involved in shape judgments was located at the edge of the LO complex (Kriegeskorte et al., 2003; James et al., 2002; Kourtzi & Kanwisher 2000; Grill-Spector et al., 1998; Van Oostende et al., 1997; Malach et al., 1995), indicating that at least parts of this complex region (Denys et al., 2002) process 3-D information about objects (Kourtzi & Kanwisher, 2001; Moore & Engel, 2001). Previous studies in passively fixating monkeys (Janssen, Vogels, & Orban, 1999, 2000) have also shown the involvement of the ventral cortex in the analysis of 3-D shape defined from stereo. In the monkey this stereo region is a restricted part of the inferotemporal cortex. The present study also suggests that only a small subpart of the LO complex, located at the edge of pITG, corresponding to the LO as generally defined by others (see Malach, Levy, & Hasson, 2002, for a review), is involved in the 3-D shape from motion processing. The major part of the LO complex is not specifically involved (Figure 8), in agreement with the results of Kourtzi and Kanwisher (2000). We refer to the most posterior and dorsal part of the LO complex as LOS. Although the LO localizer scans were performed in only three subjects, our results suggest that within LOS the 2-D shape and 2-D motion-sensitive parts behave differently and that only the motion-sensitive part is involved in 3-D shape judgements. This is reminiscent of a recent study by Murray, Olshausen, and Woods (2003), who also dissociated a motion-sensitive subregion (LOS) from two shape-sensitive parts (which they labeled LO and SLO). They observed that 3-D from motion displays activate SLO, but not LOS or LO (their terminology). The location of SLO (Murray et al., 2003) seems similar to that of the LOS part involved in 3-D shape judgements (Region 3) in our study.

The posterior IPS region overlaps the motion-sensitive region DIPSM (Sunaert et al., 1999), which has been shown to react to 3-D structure from motion stimuli (Vanduffel et al., 2002; Orban et al., 1999). On the other hand, the anterior IPS region is located ventral and anterior from another motion-sensitive region, DIPSA (Sunaert et al., 1999), also engaged by passive viewing of 3-D SFM stimuli (Vanduffel et al., 2002; Orban et al., 1999). The two IPS regions of the present study match the anterior (36, −33, 39) and posterior (+/−9, −59, 62) IPS regions involved in judging the 3-D orientation of textured surfaces (Shikata et al., 2001). The IPS region (36, −48, 54) involved in judging 3-D shape from shading (Taira, Nose, Inoue, & Tsutsui, 2001) seems located in between these two IPS regions. Finally, the anterior IPS region matches the region involved in visual 3-D object encoding (Grefkes, Weiss, Zilles, & Fink, 2002). Monkey single-cell studies have shown that neurons in the anterior part of the IPS are selective for 3-D objects (Murata, Gallese, Luppino, Kaseda, & Sakata, 2000), and those in the posterior part selective for 3-D surface orientation from stereo (Taira, Tsutsui, Jian, Yara, & Sakata, 2000) and from texture (Tsutsui, Sakata, Naganuma, & Taira, 2002). Given the functional interspecies differences recently observed (Denys et al., 2002; Vanduffel et al., 2002) or conjectured (Simon, Mangin, Cohen, Le Bihan, & Dehaene, 2002) in the intraparietal sulcus, the exact homology between these human and monkey regions is presently unclear.

Judgments of 3-D motion or surface texture, on the other hand, were found to involve exclusively or predominantly dorsal and ventral regions, respectively. These findings are more in line with the traditional distinction between the dorsal and ventral pathways (Ungerleider & Mishkin, 1982). The involvement of dorsal regions in 3-D motion judgments agrees with the results of our earlier passive study (Orban et al.,

Figure 7. Activity profiles (single-subject analysis) of 2-D motion-sensitive regions, identified by the motion localizer, plotting percent MR signal change in the five tasks compared to the average of the dimming control tasks, averaged over subjects (n = 15) and over the two hemispheres. Error bars: *SEM* from fixed-effect group analysis. Profiles of most significant voxel of LOS motion-sensitive region (A), of hMT/V5+ (C), 9 mm above (B) and 9 mm below (D) the hMT/V5+ maximum, of most significant voxel of DIPSM (E), of DIPSA (F), and 9 mm below and 3 mm anterior to the DIPSA maximum (G). 3-D SFM = 3-D shape from motion task; 3-D MOT = orientation of rotation axis task; TEX = texture task; LDC = luminance dimming detection in center; LDP = luminance dimming detection in periphery.

Figure 8. Activity profiles (single-subject analysis) of 2-D shape sensitive regions, identified by the LO complex localizer, plotting percent MR signal change in the five tasks compared to the average of the dimming control tasks, averaged over subjects (n = 3) and over the two hemispheres. Error bars: *SEM* from fixed-effect group analysis. Profiles of most significant voxel of LOS (A), posterior inferior temporal gyrus (pITG) (B), corresponding to LO, and of middle fusiform gyrus (mFG) (C) corresponding to pFG (see Malach et al., 2002, for a review). Same conventions as in Figure 7.

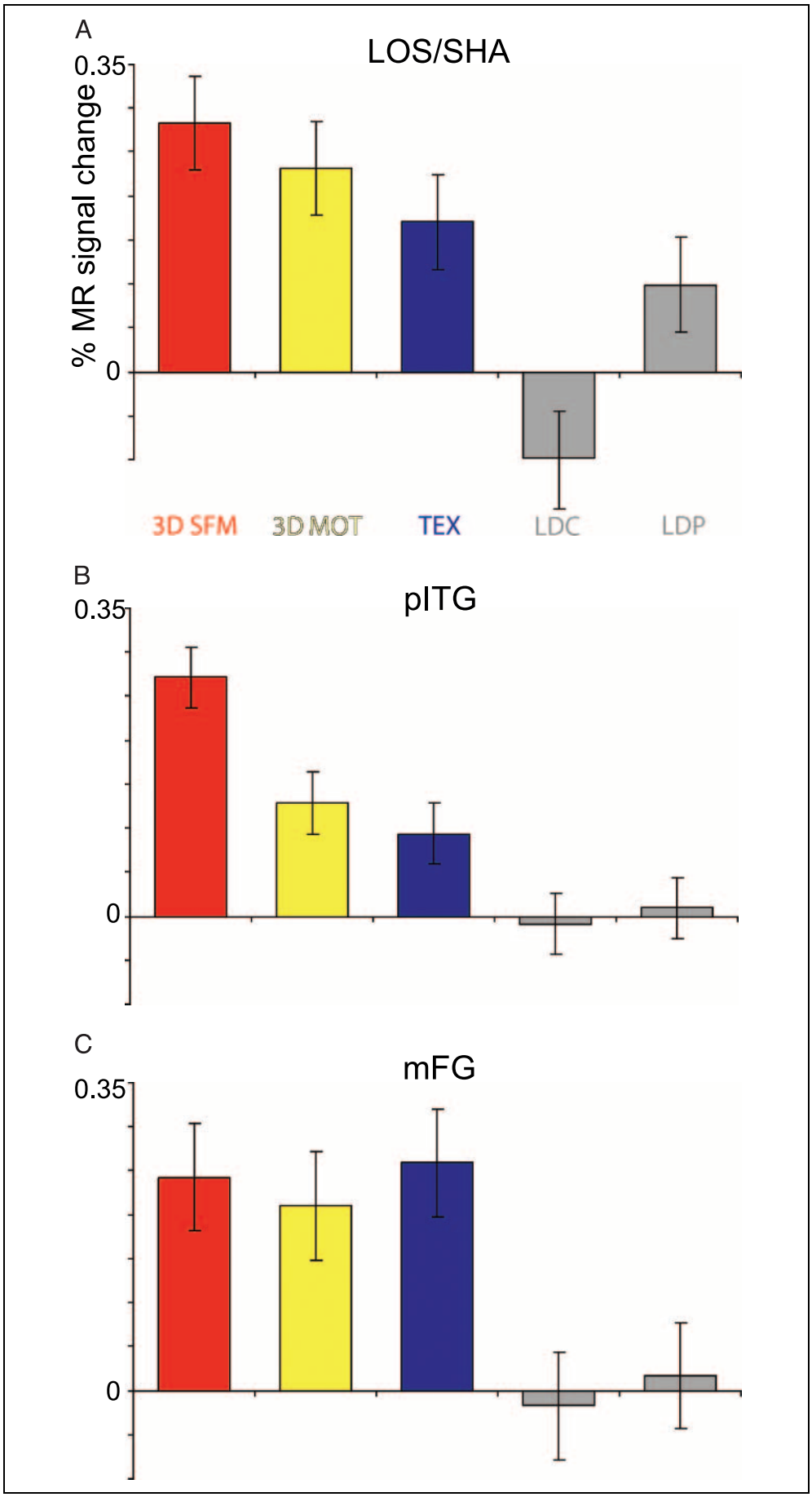

Table 2. Localization of the Specific Regions (n = 14) in the Control Experiment, with Z Scores (Fixed Effects) of Main Effects and Interactions (int)

A. Shape-Specific Regions

				SHA-MOT		*SHA-TEX*	
	x	y	z	Z[a]	Z *int*[b]	Z[a]	Z *int*[b]
R LOS	39	−81	18	>**8.0**	–	>**8.0**	–
L LOS	−36	−87	12	**7.75**	–	**6.62**	–
R ITG	36	−60	−9	3.26	–	3.95	–
L ITG	−51	−63	−12	>**8.0**	–	**5.80**	–
R posterior IPS	12	−60	72	**6.91**	–	>**8.0**	–
L posterior IPS	−18	−57	66	>**8.0**	–	>**8.0**	–

B. Shape- and Motion-Selective Regions

				SHA-TEX		*MOT-TEX*	
	x	y	z	Z[a]	Z *int*[b]	Z[a]	Z *int*[b]
R hMT/V5+	48	−63	−3	>**8.0**	3.68	>**8.0**	3.31
L hMT/V5+	−51	−69	0	>**8.0**	2.69	>**8.0**	3.29
R anterior IPS	39	−42	57	>**8.0**	–	>**8.0**	–
L anterior IPS	−42	−42	66	**5.73**	–	>**8.0**	–

C. Texture-Specific Regions

				TEX-SHA		*TEX-MOT*	
	x	y	z	Z[a]	Z *int*[b]	Z[a]	Z *int*[b]
R middle collateral sulcus	30	−54	−15		–	**5.55**	–
L middle collateral sulcus	−30	−51	−15	3.73	–	**5.73**	−2.03
L middle lingual gyrus	−18	−42	−21	4.64	–	–	–
R posterior collateral sulcus	27	−87	−21	3.14	–	4.16	–

[a]Z score main effect.

[b]Z score interaction.

1999) in which viewing the trajectory in depth of a flat object was shown to activate hMT/V5+ and an anterior IPS region. In that study, this latter activation was always weaker than that evoked by 3-D motion displays. The dorsal motion-sensitive regions along the IPS have also been shown to be activated by attentive tracking of multiple objects moving in space (Culham et al., 1999). The anterior IPS region involved in judgments of 3-D orientation of the rotation axis is close to the implicit-object-motion IPS region recently described by Kriegeskorte et al. (2003) and the PSA region described by Murray et al. (2003). In monkey, parietal neurons have been shown to represent motion trajectories (Assad & Maunsell, 1995). The involvement of ventral regions in texture judgments agrees with earlier imaging results of Puce, Allison, Asgari, Gore, & McCarthy (1996). In monkey, selectivity of inferotemporal neurons for texture has been well established (Komatsu & Ideura, 1993; Tanaka et al., 1991).

The combined involvement of the anterior ends of the respective pathways with 3-D shape and 3-D motion for the dorsal stream, and with 3-D shape and texture in the ventral stream, is in excellent agreement with the behavioral role that is typically attributed to these pathways (Goodale & Milner, 1992). In order to successfully grasp a moving object it is obviously necessary to analyze both its 3-D shape and its 3-D motion, and the successful recognition or classification of objects must clearly involve an analysis of both texture and shape information, whether 2-D or 3-D. Not surprisingly, the anterior

IPS region is close to regions involved in grasping (Simon et al., 2002; Binkofski et al., 1998, 1999), while the ITG and middle collateral sulcus regions are active in recognition (Bar et al., 2001; Grill-Spector, Kushnir, Hendler, & Malach, 2000; Rosier et al., 1999).

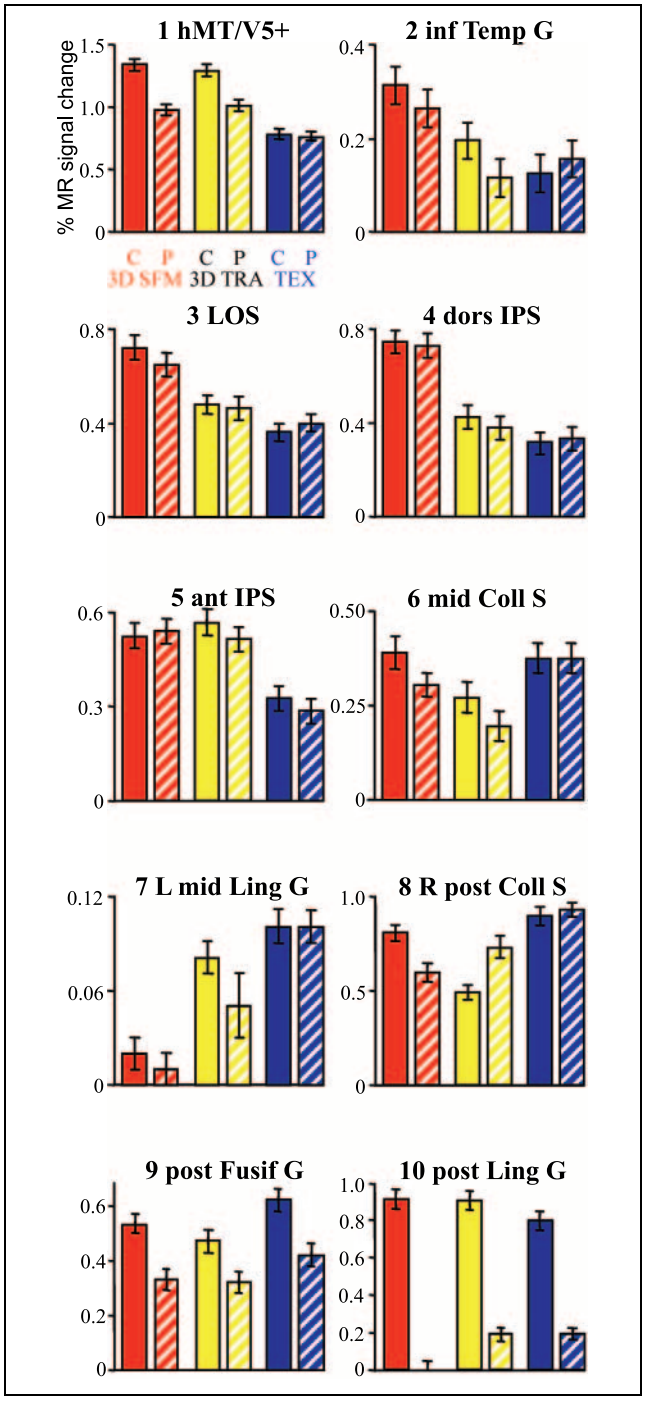

Figure 9. Activity profiles (control experiment) plotting percent MR signal change compared to fixation baseline for the 14 task-specific regions (1–8) and for two regions displaying significant spatial attention effects (9–10). Profiles 1–6 and 9–10 are averaged over the right and left hemisphere. For localization of Regions 1–8, see Table 2; coordinates Region 9: 27, −72, −15 and −24, −69, −12; and Region 10: 6, −84, −6 and −9, −84, −12. C = central; P = peripheral, other conventions as in Figure 4.

METHODS

Subjects

Fifteen healthy, right-handed human subjects (9 men, 6 women, mean age 24 years, range: 20–32) participated in the main fMRI experiment. Three subjects (3 male, mean age 25 years, range: 24–28), including 2 from the main experiment, participated in the additional control experiment. All subjects had normal or corrected-to-normal vision and no history of neurological or psychiatric disease. Subjects viewed a translucent display screen positioned in the bore of the magnet, at a distance of 36 cm from the subjects' eyes, through a mirror angled 45° to the line of sight. Subjects were instructed to fixate a point on the screen. During scanning, eye movements were recorded with an Ober2 eye-tracking system. The study was approved by the Ethical Committee of the K.U.Leuven Medical School and subjects gave their written informed consent, in accordance with the declaration of Helsinki.

Stimuli and Tasks

Stimuli were back projected onto the translucent screen using a Barco Reality 6300 (Kuurne, Belgium) projector with a spatial resolution of 1280 × 1024 pixels. Stimuli consisted of a central fixation point and two brief presentations of textured, randomly deformed spheres (Norman, Todd, & Philips, 1995) rotating back and forth, roughly 9 visual degrees in diameter (mean luminance 218 cd/m^2) on a 20 × 15 visual degrees background (Figure 1). In each trial, rotating deformed spheres were presented twice for 750 msec with an interstimulus interval of 300 msec and an intertrial interval of 1000 msec. In addition, the luminance of the central or peripheral part of the rotating spheres decreased for 200 msec in one out of two trials.

Subjects were required to make same–different judgments about the overall 3-D shape, orientation of the rotation axis, or the spatial scale of the texture by pressing a response button in the left (same) or right (different) hand. Differences in 3-D shape were created by adding a small sinusoidal perturbation in depth over the entire surface; differences in the pattern of motion were achieved by varying the amount of slant in depth of the axis of rotation; and differences in spatial scale of the texture by shifting the mean spatial frequency. Psychophysical studies have shown that for simple same–different tasks, the paired comparison strategy is optimal (Vogels & Orban, 1986). Debriefing confirmed that in the 3-D shape-discrimination task subjects indeed compared the 3-D surface characteristics of the two deformed spheres. In the main

experiment, two additional conditions were also included in which subjects were required to detect the brief luminance dimming in the central or peripheral regions of the moving object (Figure 1). Subjects pressed the left button when dimming occurred in the trial, and the right button otherwise. In the control experiment, only the three same–different tasks were included, but each of these were performed with either the central 4° of the objects in view, or with the peripheral part (outside the central 4°) visible. While in the main experiment, dimming of central or peripheral parts of the object was present in all conditions, no dimming occurred in the control experiment. It is important to emphasize that animation sequences were identical in all five response conditions of the main experiment and all three central or peripheral conditions of the control experiments. The objects presented in each pair of trial intervals were varied independently with respect to 3-D shape, 3-D motion, surface texture and, when present, central or peripheral dimming. The only systematic difference among the various conditions was the judgment an observer was required to perform.

In two training sessions prior to scanning, subjects were trained to keep fixation, and to perform the tasks for increasingly small stimulus differences or luminance decrements. A threshold was determined for each individual subject and response task so that performance could be equated at approximately 84% accuracy for all conditions.

Scanning

Functional time series consisted of 150 (main experiment) and 180 (control study) gradient EPI whole-brain scans (Siemens Sonata 1.5-T, TR/TE = 3010/50 msec, FOV 192 × 192 mm^2, 3 × 3 mm in plane resolution, 32 noncontiguous sagittal slices of 4.5-mm slice thickness with a 0.5-mm gap, Erlangen, Germany). Since more than four conditions had to be compared, a block design was considered more optimal than an event-related design. Thus, each of the five main experimental conditions were presented during epochs of 27 sec (9 whole-brain scans) and replicated once per time series. They were interspersed with baseline fixation (epochs of 18 sec) during which only the fixation point was shown. In the control experiment each time series included the six experimental conditions, 3 (tasks) × 2 (object parts), presented in 27-sec epochs (9 scans), each followed by an 18-sec fixation epoch (6 scans) and replicated once. Both in the main and control experiments, subjects received an auditory cue signaling the nature of the next task at the end of every fixation epoch. Eight time series were recorded in each subject yielding 144 whole-brain scans per condition and per subject.

In every subject, two additional time series were acquired in which passive viewing of a moving (7° diameter, 6°/sec, eight random directions) random texture pattern alternated every 10 images with the viewing of the same but stationary pattern (Sunaert et al., 1999). These runs were used to localize motion responsive areas, more specifically hMT/V5+, COS/MOT, DIPSM, and DIPSA.

Finally, anatomical images were acquired for every subject (3-D MPRAGE, TR/TE 1950/3.9 msec, TI 800 msec, FOV 240 × 256 mm^2, 240 × 256 matrix, 160-mm slab thickness, 160 sagittal partitions, 1 × 1 × 1-mm^3 voxels).

Localization of the lateral occipital complex, and more generally of areas involved in processing object shape, was done comparing passive viewing of grayscale images and image outlines versus scrambled versions of these stimuli (Kourtzi & Kanwisher, 2000, stimuli used with kind permission) in three subjects. Four time series were recorded per subject, with each series including epochs of presentations of intact grayscale images, intact outline drawings of objects, scrambled grayscale images, scrambled line drawings, and a visual baseline containing only a fixation point.

Data Analysis

Image preprocessing was done using SPM99 (Wellcome Department of Cognitive Neurology, London, UK) and included realignment, coregistration of the anatomical images to the functional scans, and spatial normalization into a standard space (Montreal Neurological Institute template) using affine and nonlinear transformations.

Functional images were spatially smoothed with a Gaussian kernel (8-mm full width at half maximum). Global changes in BOLD signal were removed by scaling; low-frequency drifts in the fMRI were removed by using high-pass filter. Condition effects were estimated by applying appropriate linear contrasts (Friston et al., 1995).

The resulting contrast images from all subjects in the main experiment were entered into a random-effects analysis per contrast, using a one-sample t test in order to create a statistical parametric map, enabling the inference based on specific contrasts to be extended to the general population (Friston, Holmes, & Worsley, 1999). This random-effects analysis was restricted a priori to visually responsive voxels, i.e., voxels reaching $p < .001$ uncorrected in the contrast of all active conditions minus fixation only. In the main analysis, the three discrimination conditions were compared pairwise, yielding six contrasts. The results of these comparisons were color-coded using a triangular scheme. Colors at the endpoints of the triangle in Figures 2 and 4 denote significant activation ($p < .001$ uncorrected for multiple comparisons, restricted to visually responsive voxels) of one condition compared to both the other conditions; middle colors denote activation in common to two conditions relative to the remaining condition. Only regions ($n = 13$) in which local maxima reached $p < .05$ corrected for multiple

comparisons (for visually responsive voxels) at least in one of the six subtractions, were considered further. In an additional analysis, all three discrimination tasks were compared to the two dimming detection tasks. Also, conditions in which central or peripheral dimming was attended were compared. These contrasts yielded voxels in which visuospatial attention had a significant effect ($p < .001$ uncorrected). Finally, the main experiment was also subjected to a single-subject analysis. For single subjects the level of significance was set at $p < .001$ uncorrected.

A fixed-effect analysis was performed on the data of the control experiment. As in the analysis of the main experiment, the three discrimination conditions were compared pairwise, yielding six contrasts, but data were averaged over central and peripheral presentations.

Acknowledgments

The authors are indebted to Y. Celis, P. Kayenbergh, G. Meulemans, M. De Paep, and W. Depuydt for technical help. This study was supported by GOA 2000/11, FWO G.0202.99, G.0401.00, and GSKE. H. P. is a research assistant of the FWO.

Reprint requests should be sent to Guy A. Orban, K. U. Leuven, Medical School, Laboratorium Neuro- en Psychofysiologie, Campus Gasthuisberg, B-3000 Leuven, Belgium.

The data reported in this experiment have been deposited in the fMRI Data Center (http://www.fmridc.org). The accession number is 2-2003-114DG.

REFERENCES

Aguirre, G. K., & D'Esposito, M. (1997). Experimental knowledge is subserved by separable dorsal/ventral neural areas. *Journal of Neuroscience, 17,* 2512–2518.

Assad, J. A., & Maunsell, J. H. (1995). Neuronal correlates of inferred motion in primate posterior parietal cortex. *Nature, 373,* 518–521.

Bar, M., Tootell, R. B., Schacter, D. L., Greve, D. N., Fischl, B., Mendola, J. D., Rosen, B. R., & Dale, A. M. (2001). Cortical mechanisms specific to explicit visual object recognition. *Neuron, 29,* 529–535.

Binkofski, F., Buccino, G., Posse, S., Seitz, R. J., Rizzolatti, G., & Freund, H. (1999). A fronto-parietal circuit for object manipulation in man: Evidence from an fMRI study. *European Journal of Neuroscience, 11,* 3276–3286.

Binkofski, F., Dohle, C., Posse, S., Stephan, K. M., Hefter, H., Seitz, R. J., & Freund, H. J. (1998). Human anterior intraparietal area subserves prehension: A combined lesion and functional MRI activation study. *Neurology, 50,* 1253–1259.

Bradley, D. C., Chang, G. C., & Andersen, R. A. (1998). Encoding of three-dimensional structure-from-motion by primate area MT neurons. *Nature, 392,* 714–717.

Brefczynski, J. A., & DeYoe, E. A. (1999). A physiological correlate of the ''spotlight'' of visual attention. *Nature Neuroscience, 2,* 370–374.

Corbetta, M., Akbudak, E., Conturo, T. E., Snyder, A. Z., Ollinger, J. M., Drury, H. A., Linenweber, M. R., Petersen, S. E., Raichle, M. E., Van Essen, D. C., & Shulman, G. L. (1998). A common network of functional areas for attention and eye movements. *Neuron, 21,* 761–773.

Corbetta, M., Miezin, F. M., Dobmeyer, S., Shulman, G. L., & Petersen, S. E. (1991). Selective and divided attention during visual discriminations of shape, color, and speed: Functional anatomy by positron emission tomography. *Journal of Neuroscience, 11,* 2383–2402.

Corbetta, M., Miezin, F. M., Shulman, G. L., & Petersen, S. E. (1993). A PET study of visuospatial attention. *Journal of Neuroscience, 13,* 1202–1226.

Cornette, L., Dupont, P., Bormans, G., Mortelmans, L., & Orban, G. A. (2001). Separate neural correlates for the mnemonic components of successive discrimination and working memory tasks. *Cerebral Cortex, 11,* 59–72.

Cornette, L., Dupont, P., Rosier, A., Sunaert, S., Van Hecke, P., Michiels, J., Mortelmans, L., & Orban, G. A. (1998). Human brain regions involved in direction discrimination. *Journal of Neurophysiology, 79,* 2749–2765.

Culham, J. C., Dukelow, S. P., Vilis, T., Hassard, F. A., Gati, J. S., Menon, R. S., & Goodale, M. A. (1999). Recovery of fMRI activation in motion area MT following storage of the motion aftereffect. *Journal of Neurophysiology, 81,* 388–393.

Denys, K., Vanduffel, W., Fize, D., Peuskens, H., Nelissen, K., Vandenberghe, R., & Orban, G. A. (2002). The lateral occipital complex in the monkey and the human. *Society for Neuroscience Abstracts,* 161.1.

Dupont, P., Orban, G. A., De Bruyn, B., Verbruggen, A., & Mortelmans, L. (1994). Many areas in the human brain respond to visual motion. *Journal of Neurophysiology, 72,* 1420–1424.

Faillenot, I., Sunaert, S., Van Hecke, P., & Orban, G. A. (2001). Orientation discrimination of objects and gratings compared: An fMRI study. *European Journal of Neuroscience, 13,* 585–596.

Faillenot, I., Toni, I., Decety, J., Gregoire, M. C., & Jeannerod, M. (1997). Visual pathways for object-oriented action and object recognition: Functional anatomy with PET. *Cerebral Cortex, 7,* 77–85.

Fias, W., Dupont, P., Reynvoet, B., & Orban, G. A. (2002). The quantitative nature of a visual task differentiates between ventral and dorsal stream. *Journal of Cognitive Neuroscience, 14,* 646–658.

Friston, K. J., Holmes, A. P., Poline, J. B., Grasby, P. J., Williams, S. C., Frackowiak, R. S., & Turner, R. (1995). Analysis of fMRI time-series revisited. *Neuroimage, 2,* 45–53.

Friston, K. J., Holmes, A. P., & Worsley, K. J. (1999). How many subjects constitute a study? *Neuroimage, 10,* 1–5.

Goodale, M. A., & Milner, A. D. (1992). Separate visual pathways for perception and action. *Trends in Neuroscience, 15,* 20–25.

Grefkes, C., Weiss, P. H., Zilles, K., & Fink, G. R. (2002). Crossmodal processing of object features in human anterior intraparietal cortex: An fMRI study implies equivalencies between humans and monkeys. *Neuron, 35,* 173–184.

Grill-Spector, K., Kushnir, T., Hendler, T., Edelman, S., Itzchak, Y., & Malach, R. (1998). A sequence of object-processing stages revealed by fMRI in the human occipital lobe. *Human Brain Mapping, 6,* 316–328.

Grill-Spector, K., Kushnir, T., Hendler, T., & Malach, R. (2000). The dynamics of object-selective activation correlate with recognition performance in humans. *Nature Neuroscience, 3,* 837–843.

Gross, C. G., Rocha-Miranda, C. E., & Bender, D. B. (1972). Visual properties of neurons in inferotemporal cortex of the Macaque. *Journal of Neurophysiology, 35,* 96–111.

Grünewald, A., Bradley, D. C., & Andersen, R. A. (2002). Neural correlates of structure-from-motion perception in macaque V1 and MT. *Journal of Neuroscience, 22,* 6195–6207.

Haxby, J. V., Horwitz, B., Ungerleider, L. G., Maisog, J. M., Pietrini, P., & Grady, C. L. (1994). The functional organization of human extrastriate cortex: A PET-rCBF study of selective attention to faces and locations. *Journal of Neuroscience, 14,* 6336–6353.

James, T. W., Humphrey, G. K., Gati, J. S., Menon, R. S., & Goodale, M. A. (2002). Differential effects of viewpoint on object-driven activation in dorsal and ventral streams. *Neuron, 35,* 793–801.

Janssen, P., Vogels, R., & Orban, G. A. (1999). Macaque inferior temporal neurons are selective for disparity-defined three-dimensional shapes. *Proceedings of the National Academy of Sciences, U.S.A., 96,* 8217–8222.

Janssen, P., Vogels, R., & Orban, G. A. (2000). Selectivity for 3D shape that reveals distinct areas within macaque inferior temporal cortex. *Science, 288,* 2054–2056.

Komatsu, H., & Ideura, Y. (1993). Relationships between color, shape, and pattern selectivities of neurons in the inferior temporal cortex of the monkey. *Journal of Neurophysiology, 70,* 677–694.

Kourtzi, Z., Bulthoff, H. H., Erb, M., & Grodd, W. (2002). Object-selective responses in the human motion area MT/MST. *Nature Neuroscience, 5,* 17–18.

Kourtzi, Z., & Kanwisher, N. (2000). Cortical regions involved in perceiving object shape. *Journal of Neuroscience, 20,* 3310–3318.

Kourtzi, Z., & Kanwisher, N. (2001). Representation of perceived object shape by the human lateral occipital complex. *Science, 293,* 1506–1509.

Kovács, G., Vogels, R., & Orban, G. A. (1995). Selectivity of macaque inferior temporal neurons for partially occluded shapes. *Journal of Neuroscience, 15,* 1984–1997.

Kriegeskorte, N., Sorger, B., Naumer, M., Schwarzbach, J., van den Boogert, E., Hussy, W., & Goebel, R. (2003). Human cortical object recognition from a visual motion flowfield. *Journal of Neuroscience, 15,* 1451–1463.

Logothetis, N. K., & Pauls, J. (1995). Psychophysical and physiological evidence for viewer-centered object representations in the primate. *Cerebral Cortex, 5,* 270–288.

Malach, R., Levy, I., & Hasson, U. (2002). The topography of high-order human object areas. *Trends in Cognitive Sciences, 6,* 176–184.

Malach, R., Reppas, J. B., Benson, R. R., Kwong, K. K., Jiang, H., Kennedy, W. A., Ledden, P. J., Brady, T. J., Rosen, B. R., & Tootell, R. B. H. (1995). Object-related activity revealed by functional magnetic resonance imaging in human occipital cortex. *Proceedings of the National Academy of Sciences, U.S.A., 92,* 8135–8139.

Moore, C., & Engel, S. A. (2001). Neural response to perception of volume in the lateral occipital complex. *Neuron, 29,* 277.

Murata, A., Gallese, V., Luppino, G., Kaseda, M., & Sakata, H. (2000). Selectivity for the shape, size, and orientation of objects for grasping in neurons of monkey parietal area AIP. *Journal of Neurophysiology, 83,* 2580–2601.

Murray, S. O., Olshausen, B. A., & Woods, D. L. (2003) Processing shape, motion end three-dimensional shape-from-motion in the human cortex. *Cerebral Cortex, 13,* 508–516.

Nobre, A. C., Sebestyen, G. N., Gitelman, D. R., Mesulam, M. M., Frackowiak, R. S. J., & Frith, C. D. (1997). Functional localization of the system for visuospatial attention using positron emission tomography. *Brain, 120,* 515–533.

Norman, J. F., Todd, J. T., & Orban, G. A. (2001). The perception and discrimination of global 3-D shape from the deformations of texture, shading, and specular highlights. *Journal of Vision, 1,* 392a.

Norman, J. F., Todd, J. T., & Philips, F. (1995). The perception of surface orientation from multiple sources of optical information. *Perception and Psychophysics, 57,* 629–636.

O'Craven, K. M., Downing, P. E., & Kanwisher, N. (1999). fMRI evidence for objects as the units of attentional selection. *Nature, 401,* 584–587.

Orban, G. A., Dupont, P., De Bruyn, B., Vandenberghe, R., Rosier, A., & Mortelmans, L. (1998). Human brain activity related to speed discrimination tasks. *Experimental Brain Research, 122,* 9–22.

Orban, G. A., Dupont, P., Vogels, R., Bormans, G., & Mortelmans, L. (1997). Human brain activity related to orientation discrimination tasks. *European Journal of Neuroscience, 9,* 246–259.

Orban, G. A., Sunaert, S., Todd, J., T., Van Hecke, P., & Marchal, G. (1999). Human cortical regions involved in extracting depth from motion. *Neuron, 24,* 929–940.

Paradis, A. L., Cornilleau-Pérès, V., Droulez, J. Van De Moortele, P. F., Lobel, E., Berthoz, A., Le Bihan, D., & Poline, J. B. (2000). Visual perception of motion and 3-D structure from motion: An fMRI study. *Cerebral Cortex, 10,* 772–783.

Peuskens, H., Sunaert, S., Dupont, P., Van Hecke, P., & Orban, G. A. (2001). Human brain regions involved in heading estimation. *Journal of Neuroscience, 21,* 2451–2461.

Puce, A., Allison, T., Asgari, M., Gore, J. C., & McCarthy, G. M. (1996). Differential sensitivity of human visual cortex to faces, letter strings, and textures: A functional magnetic resonance imaging study. *Journal of Neuroscience, 16,* 5205–5215.

Rosier, A. M., Cornette, L., Dupont, P., Bormans, G., Mortelmans, L., & Orban, G. A. (1999). Regional brain activity during shape recognition impaired by a scopolamine challenge to encoding. *European Journal of Neuroscience, 11,* 3701–3714.

Sereno, A. B., & Maunsell, J. H. (1998). Shape selectivity in primate lateral intraparietal cortex. *Nature, 395,* 500–503.

Sereno, M. E., Trinath, T., Augath, M., & Logothetis, N. K. (2002). Three-dimensional shape representation in monkey cortex. *Neuron, 33,* 635–652.

Shikata, E., Hamzei, F., Glauche, V., Knab, R., Dettmers, C., Weiller, C., & Büchel, C. (2001). Surface orientation discrimination activates caudal and anterior intraparietal sulcus in humans: An event-related fMRI study. *Journal of Neurophysiology, 85,* 1309–1314.

Simon, O., Mangin, J.-F., Cohen, L., Le Bihan, D., & Dehaene, S. (2002). Topographical layout of hand, eye, calculation, and language-related areas in the human parietal lobe. *Neuron, 33,* 475–487.

Sunaert, S., Van Hecke, P., Marchal, G., & Orban, G. A. (1999). Motion-responsive regions of the human brain. *Experimental Brain Research, 127,* 355–370.

Taira, M., Nose, I., Inoue, K., & Tsutsui, K. I. (2001). Cortical areas related to attention to 3D surface structures based on shading: An fMRI study. *Neuroimage, 14,* 959–966.

Taira, M., Tsutsui, K. I., Jiang, M., Yara, K., & Sakata, H. (2000). Parietal neurons represent surface orientation from the gradient of binocular disparity. *Journal of Neurophysiology, 83,* 3140–3146.

Tanaka, K., Saito, H., Fukada, Y., & Moriya, M. (1991). Coding visual images of objects in the inferotemporal cortex of the macaque monkey. *Journal of Neurophysiology, 66,* 170–189.

Todd, J. T., & Norman, J. F. (1991). The visual perception of smoothly curved surfaces from minimal apparent motion sequences. *Perception & Psychophysics, 50,* 509–523.

Tolias, A. S., Smirnakis, S. M., Augath, M. A., Trinath, T., &

Logothetis, N. K. (2001). Motion processing in the macaque: Revisited with functional magnetic resonance imaging. *Journal of Neuroscience, 21,* 8594–8601.
Tootell, R. B., Reppas, J. B., Kwong, K. K., Malach, R., Born, R. T., Brady, T. J., Rosen, B. R., & Belliveau, J. W. (1995). Functional analysis of human MT and related visual cortical areas using magnetic resonance imaging. *Journal of Neuroscience, 15,* 3215–3230.
Tootell, R. B. H., Hadjikhani, N., Hall, E. K., Marrett, S., Vanduffel, W., Vaughan, J. T., & Dale, A. M. (1998). The retinotopy of visual spatial attention. *Neuron, 21,* 1409.
Treue, S., & Martinez Trujillo, J. C. (1999). Feature-based attention influences motion processing gain in macaque visual cortex. *Nature, 399,* 575–579.
Tsutsui, K. I., Sakata, H., Naganuma, T., & Taira, M. (2002). Neural correlates for perception of 3D surface orientation from texture gradient. *Science, 298,* 409–412.
Ullman, S. (1979). *The interpretation of visual motion.* Cambridge: MIT Press.
Ungerleider, L. G., & Mishkin, M. (1982). Two cortical visual systems. In D. J. Ingle, M. A. Goodale, & R. J. W. Mansfield (Eds.), *Analysis of visual behavior* (pp. 549–586). Cambridge: MIT Press.
Vandenberghe, R., Dupont, P., De Bruyn, B., Bormans, G., Michiels, J., Mortelmans, L., & Orban, G. A. (1996). The influence of stimulus location on the brain activation pattern in detection and orientation discrimination. A PET study of visual attention. *Brain, 119,* 1263–1276.
Vanduffel, W., Fize, D., Mandeville, J. B., Nelissen, K., Van Hecke, P., Rosen, B. R., Tootell, R. B. H., & Orban, G. A. (2001). Visual motion processing investigated using contrast agent-enhanced fMRI in awake behaving monkeys. *Neuron, 32,* 565–577.
Vanduffel, W., Fize, D., Peuskens, H., Denys, K., Sunaert, S., Todd, J. T., & Orban, G. A. (2002). Extracting 3D from motion: Differences in human and monkey intraparietal cortex. *Science, 298,* 413–415.
Van Oostende, S., Sunaert, S., Van Hecke, P., Marchal, G., & Orban, G. A. (1997). The kinetic occipital (KO) region in man: An fMRI study. *Cerebral Cortex, 7,* 690–701.
Vogels, R., & Orban, G. A. (1986). Decision processes in visual discrimination of line orientation. *Journal of Experimental Psychology: Human Perception and Performance,* 12, 115–132.
Wallach, H., & O'Connell, D. N. (1953). The kinetic depth effect. *Journal of Experimental Psychology, 45,* 205–217.
Watson, J. D. G., Myers, R., Frackowiak, R. S. J., Hajnal, J. V., Woods, R. P., Mazziota, J. C., Shipp S., & Zeki S. (1993). Area V5 of the human brain: Evidence from a combined study using positron emission tomography and magnetic resonance imaging. *Cerebral Cortex, 3,* 79–94.
Xiao, D. K., Marcar, V. L., Raiguel, S. E., & Orban, G. A. (1997). Selectivity of macaque MT/V5 neurons for surface orientation in depth specified by motion. *European Journal of Neuroscience, 9,* 956–964.
Zeki, S., Watson, J. D., Lueck, C. J., Friston, K. J., Kennard, C., & Frackowiak, R. S. (1991). A direct demonstration of functional specialization in human visual cortex. *Journal of Neuroscience, 11,* 641–649.